

Antibody@Silica Coated Iron Oxide Nanoparticles: Synthesis, Capture of *E. coli* and SERS Titration of Biomolecules with Antibacterial Silver Colloid

Shiva K. Rastogi^{1*}, Jamie M. F. Jabal², Huijin Zhang³, Charlene M. Gibson¹, Kevin J. Haler⁴, You Qiang³, D. Eric Aston² and A. Larry Branen⁴

¹Department of Chemistry, University of Idaho, Moscow, ID - 83844-2343

²Department of Chemical and Materials Engineering, University of Idaho, Moscow, ID - 83844, USA

³Departmental of Physics and Environmental Science Program, University of Idaho, Moscow, ID - 83844, USA

⁴Biosensors and Nanotechnology Applications Laboratory, University of Idaho, 1031 N Academic Way, Coeur d'Alene, ID - 83814, USA

Abstract

Silica coated iron oxide ($\text{SiO}_2/\text{Fe}_3\text{O}_4 + \gamma\text{-Fe}_2\text{O}_3$) nanoparticles (SIO-NPs; 75 ± 10 nm in diameter) were prepared by encapsulation of iron oxide NPs with silica using sol-gel method and characterized through spectroscopy methods. The SIO NPs were chemically activated by cyanogens bromide and then functionalized with *Escherichia coli* (*E. coli*) antibodies. These immuno-magnetic (IM NPs) were used to capture and concentrate *E. coli* from ~ 180 cfu/mL suspension. The identification of bacteria was performed by plating on nutrient agar, fluorescent microscopy and scanning electron microscopy. Surface enhanced Raman spectroscopy (SERS) was used to identify different biomolecules of bacterial cell upon the interaction of colloidal silver nanoparticle (Ag NPs 6 ± 4 nm) at different period of time. In our previous report we demonstrated the antibacterial property of colloidal Ag NPs. Therefore, current approach, using IM, and Ag NPs and SERS, provide detailed molecular identification of *E. coli* as Ag NPs interact over the time. This method would be applicable for food safety, environment protection, biological threat material, antibacterial and other routine *E. coli* identification projects.

Keywords: Silica; Iron oxide; Antibody; *Escherichia coli*; Electron microscopy; Raman spectroscopy

Introduction

The quick and reliable identification of microorganisms is critical for the proper cure of infected individuals [1]. There are adequate conventional methods available for microbial identification [2]. However, most of them are laborious and expensive. To overcome from time-consuming methods, spectroscopic methods like fluorescence [3,4], mass spectroscopy [5], Infrared (IR) spectroscopy [6] and surface-enhanced Raman spectroscopy (SERS) [7,8] have been developed. These techniques are capable of identifying a whole microorganism from a limited number of microbial cells in a non-destructive manner.

Among the spectroscopic methods, SERS has drawn attention because it is compatible with biological samples, requires lesser sample preparation and provide signals with detailed information concerning microorganism [9]. Therefore, SERS, as an analytical tool, has been used in biological applications such as immunoassay [10], cellular studies [11], cancer diagnostic [12], bacterial detection [13], and food-safety projects [14] etc. For achieving significant information from bacterial cell using SERS, colloidal gold (Au) or silver (Ag) is required [15].

There, are several reports published concerning that the detection of a biomarker belongs to photogenic bacterial species on a noble surface. A report has been published by Efrima et al. [16] on SERS study of the cell wall with Ag nanoparticles (NPs) by reducing silver ions in the presence of bacteria. They also demonstrated that the SERS spectra obtained from the bacterium cell walls and inside the bacterium were different when Ag NPs enter inside the bacterium cell [16].

Commonly, to capture, separate and identify a bacterium from a contaminated sample immunosensor is one of the choices. A typical immunosensor is usually fabricated by immobilizing the specific antibody on the surface of an inert solid support via chemical or physical mechanisms [17]. In general, chemical immobilization can provides strong and stable protein attachment but physical adsorption provides only short time activity retention. Though, non-porous iron oxides (Fe_3O_4 and $\gamma\text{-Fe}_2\text{O}_3$) nanoparticles (IO-NPs), as a solid support,

suffer from the drawback that some inactivation process for protein may be possible [18], the IO NPs possess their unique magnetic property – super paramagnetism, which enables their stability and dispersion after removing the magnetic. Hence, silica coated IO NPs (SIO NPs) not only offer improved stability but also help to bind the various chemical and biological ligands covalently at the surface of NPs [19].

Several interesting and important articles have been reported for SERS based identification and rapid detection of *E. coli* using immune-magnetic IM NPs and others methods. Guven et al. [8] has reported the use of IM separation and SERS for rapidly (less than 70 min) and sensitively detect *E. coli* in real water sample using rod shaped Au NPs [8]. Liu et al. [14] have reported the feasibility of citrate reduced colloidal Ag SERS for differentiating three important food borne pathogens (*E. coli*, *Listeria monocytogenes*, and *Salmonella typhimurium*) [20]. In another article, a convective assembly method has been reported by Kahraman et al. [21] for uniform bacterial (Gram-negative and Gram-positive bacterium) sample preparation. This method deposited bacteria and Ag NPs on a glass slide as a thin film in an ordered structure and detect using SERS, avoiding spot-to-spot variations [21]. These reports clearly demonstrated that the IM NPs can be effectively used to capture bacteria, and citrate reduced Ag NPs are sufficient for SERS identification on glass slide. But, no report

***Corresponding author:** Shiva K. Rastogi, Department of Chemistry, University of Idaho, Moscow, ID - 83844-2343, Tel: 1-208-758-0416; Fax: 1-208-885-6173; E-mail: srastogi@uidaho.edu

Received November 06, 2011; **Accepted** November 26, 2011; **Published** November 29, 2011

Citation: Rastogi SK, Jabal JMF, Zhang H, Gibson CM, Haler KJ, et al. (2011) Antibody@Silica Coated Iron Oxide Nanoparticles: Synthesis, Capture of *E. coli* and SERS Titration of Biomolecules with Antibacterial Silver Colloid. J Nanomedic Nanotechnol 2:121. doi:10.4172/2157-7439.1000121

Copyright: © 2011 Rastogi SK, et al. This is an open-access article distributed under the terms of the Creative Commons Attribution License, which permits unrestricted use, distribution, and reproduction in any medium, provided the original author and source are credited.

has explained what an optimum time period of incubation required for identification of a particular biomolecule of *E. coli* would be and if the sample is incubated for longer time with Ag NPs then how it will affect on SERS signals.

In our previous report we have shown the synthesis and application of colloidal Ag NPs and Ag cluster over silica NPs for antibacterial activity [22]. Further, in order to identify the different biomolecules upon the action of Ag NPs on bacterial cells, here we synthesized and characterized SIO NPs. The surface hydroxyl groups of these NPs were activated for covalent immobilization of *E. coli* antibody. These IM NPs were used to capture magnetic separation and concentrate *E. coli* from phosphate buffer saline (PBS) suspension as shown in scheme 1. The captured *E. coli* were treated with colloidal Ag NPs more than 20 h and performed SERS at different time intervals to identify different biomolecules of *E. coli*.

Experimental

Material and chemicals

All the chemicals and reagents were purchased from Sigma Aldrich, (St. Louis, MO, USA) and Fisher Scientific (New Jersey, USA). Polyclonal general goat anti-*E. coli* antibody was purchased from Viro Stat Inc. (Portland, ME, USA) and Invitrogen molecular probes (Eugene, Oregon, USA). Luria Bertani (LB) medium and agar were purchased from EMD chemicals, (Darmstadt, Germany). General strains of environmental *E. coli* were isolated from local fresh water streams, *E. coli* strain ATCC 25922 general strains were provided by Dr. Gregory Bohach (MMBB Department, Univ. of Idaho (UI), Moscow, Idaho, USA). The buffer: phosphate buffered saline (PBS) was prepared from a 10x autoclaved stock (10x PBS: 100 mM phosphate buffer, 1.37M NaCl, 27 mM KCl, pH 7.2. Deionized (DI; 18.2 M Ω) water was collected from Labconco, water Pro PS.

Instrumentation

JEOL 1200EX II model was used for transmission electron microscopic (TEM) images and Supera Gemini 35 VP FE-SEM (Zeiss) coupled with Thermolectron (Zeiss) model was used for Field emission scanning electron microscopic (FE-SEM) imaging. The functional

group of the nanoparticles was characterized using Fourier transform-infrared (FT-IR) and Ultraviolet visible (UV-vis) spectrophotometer (model; PharmaSpec UV-1700). Bacterial growth was monitored by plating on agar plates. Bactericidal effects were characterized using a fluorescent microscope (Leitz LaborLux S) with a Leica EC3 objective head and digital camera and a Leo fluorescent Lamp. All glassware was cleaned with aqua-regia and rinsed with ethanol and DI water several times before use.

Visible Raman and SERS spectra were recorded using a Raman analyzer WITec alpha300 Raman Microscopy System (WITec GmbH, Ulm, Germany) equipped with 532 nm and 785 nm excitations. An integrated confocal microscope, with a 100x objective, was used to focus the laser and obtain an optimal SERS response. The laser power was used in the range of 0.04 - 2 mW, and the exposure time was 0.5 to 3 sec for comparative purposes. The WITech control ver. 1.5 software package (WITec GmbH, Ulm, Germany) running under Windows XP was used of the instrument control and data acquisition.

Synthesis of iron oxide ($\text{Fe}_3\text{O}_4 + \gamma\text{-Fe}_2\text{O}_3$) nanoparticles (IO-NPs)

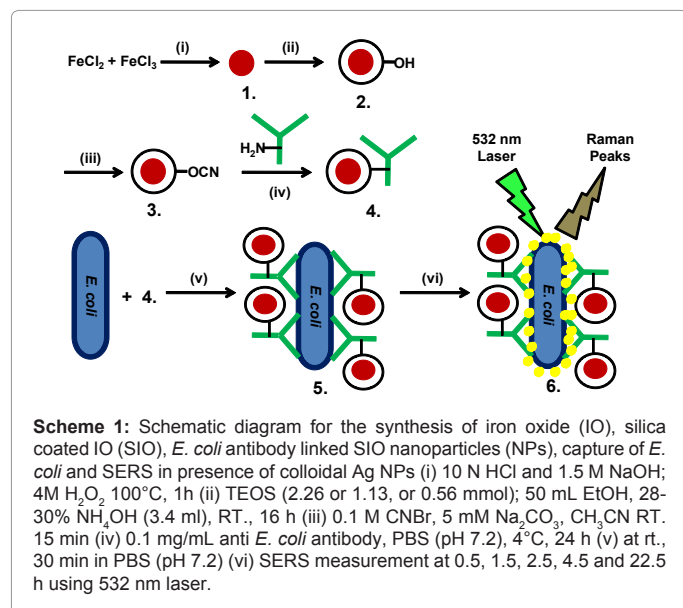
The synthesis of IO NPs was carried out using previously reported method [23,24]. FeCl_2 (0.5g; 15.78 mmol) and FeCl_3 (1.3g; 8.01 mmol) were dissolved into deoxygenated DI water (deox-DIW; 6.25 mL) and 0.212 mL of 10N HCl. The above solution was added drop wise into 62.5 ml of 1.5M NaOH (in deox-DIW) over the period of 2 h, with vigorous stirring (1500 rpm). The reaction mixture was stirred overnight at room temperature (RT). After completion of time black precipitate (ppt) was hold by bar magnet and aqueous layer was decanted and ppt was washed three times with deox-DIW and finally suspended into 75 mL of DIW. The above suspension was oxidized with 4M H_2O_2 at 100°C for 1 hr with air bubbling. The black color turned into dark brown. The brown ppt was separated using magnet and washed three times with DIW and the ppt was dried in desiccated under vacuum for 24 hr at RT. These brown color mixtures of iron oxide ($\text{Fe}_3\text{O}_4 + \gamma\text{Fe}_2\text{O}_3$) were analyzed for magnetite property and through TEM imaging, which gave needle shape structures.

General method for silica coated iron oxide nanoparticles (SIO-NPs)

50 mL of ethylalcohol (EtOH) 200 proof, 1 mL of DI water and required amount for 2a, 2b and 2c SIO NPs (2.26 or 1.13, or 0.56 mmol) tetraethylorthosilicate (TEOS) respectively were mixed into 125 mL round bottom flask and stirred for 30 min. 3.4 mL of ammonium hydroxide (28-30%) solution was added to above solution and stirred at 1500 rpm for 20 min. at RT. The magnetite particles (25 mg) suspension in 2 mL of DIW and EtOH (v/v; 1:1) was added drop wise with vigorous stirring over the period of 30 min. The reaction was allowed to stir for 16 h at RT. The brown suspension was separated through magnet and washed with 80% EtOH three times and then cured in vacuum oven at 110°C for 24 h.

Determination of magnetic property

Magnetic properties of IO and SIO NPs samples were measured by placing the dry and weighted powdered sample (~10 mg) in vibrating sample magnetometer (VSM; DMS model 1660) at RT. Magnetic hysteresis curve (saturation magnetization vs coercivity) for each samples was recorder by applying magnetic field of -13500 Oe to 13500 Oe.



Activation of SIO NPs with cyanogen bromide

5 mg of SIO NPs were suspended into 10 mL of 5 mM Na_2CO_3 solution. A solution of cyanogens bromide (CNBr) in acetonitrile (0.1 M) was then added drop wise under stirring for 15 min. at RT. The activated SIO NPs were washed twice with ice-cold DIW and then stored into PBS buffer (pH 6.8).

Conjugation NPs with antibody

10 μL of polyclonal goat anti-*E. coli* antibody (0.1 mg/mL) in PBS buffer (pH 7.2) was added to the activated SIO NPs (1mL; 0.5 mg) and mixed through radial rotor for 24 h at 4°C. The particles were treated with 1% BSA (blocking buffer) for 1h and the final product was washed and re-suspended in PBS buffer (pH 7.2).

To analyzed the yield of this reaction, the SIO-antibody conjugate (1 mL in PBS), before adding 1% BSA, centrifuged at 14000 g for 20 min. Supernatant was removed and particle conjugate was suspended in 0.05M aq NaOH solution (1 mL; pH 10.0) and mixed on radial rotor for 24 h at rt. The suspension was centrifuged again at 14000 g for 20 min. and UV-visible absorption reading was measured at 260 nm. The final loading of the antibody come 0.22 μg /0.5 mg SIO NPs (yield 22%), which is equal to 440 μg of antibody per 1 g of SIO NPs.

E. coli culture

E. coli were cultured on in LB (Luria Bertani) growth media in tubes [Figure 3a] at 37°C for 24 h in our lab as reported earlier [22]. Serial dilutions up to 10^{-9} concentration *E. coli* culture were prepared in a total volume of 1 mL of in PBS (pH 7.2). 100 μL of each bacterial suspension was placed on sterile LB agar plates. The plates were incubated at 37°C for 24 h followed by the counting the number colony forming units [cfu/mL; Figure 3b].

E. coli capture and concentration using NP

The NPs 4 (25 $\mu\text{g}/\text{mL}$) were mixed in bacterial suspension from its different dilutions (10^{-6} - 10^{-9}) containing $\sim 1.8 \times 10^4$ to ~ 18 cfu/mL and set up on cyclic rotator for 30 min at rt. Then the NPs were magnetically separated from the bacterial suspension and washed twice with PBS containing 0.1% Tween 20 (PBST). A small aliquot (50 μL) of the washed NPs with bacteria were placed on a sterile LB agar plate and incubated for 12 hr at 37°C to confirm the presence of bacteria. The remaining aliquots of the samples were used for other analyses.

Fluorescent microscopy of captured *E. coli* with NPs

The captured *E. coli* bacteria and NP 4 complex, respectively was rinsed three times using 1 mL of sterile 0.85% NaCl solution. Then the bacteria complex were re-suspended in 1 mL 0.85% NaCl solution and 3 μL of an equal part mixture of reagents A and B from the LIVE/DEAD BacLight bacterial viability kit were added. The suspension was incubated at RT for 15 min, followed by a filtration onto a 25 mm black polycarbonate filter paper. The filter was then placed onto glass microscope slide with cover slips and visualized under a fluorescent microscope using a 63X oil immersion fluorescent lens using green filters for analysis. We have successfully used this procedure for staining only the *E. coli* in our previous study [22].

Raman identification

Each aqueous sample (0.2 - 0.5 μL) was placed on glass slide and dried at RT before taking the Raman spectra. The laser beam was focused on a 2 μm area of each sample to image and acquire the Raman spectra. The microscope was used to localize the bacteria. Each

spectrum took ~ 5 min to acquire. The performance of the 532 nm lasers was found to be superior for bacterial SERS study over 785 nm laser (data not shown here) in the presence of Ag NPs. For assessing the reproducibility of this approach, three replicate spectra were obtained from each sample from different points of the matrix were taken, focusing on the different spots.

Result and discussion

Nanoparticles synthesis and characterization

TEM image of irregularly shaped IO NPs of 15 ± 4 nm of size but needle like structures with length of 90 ± 10 nm and width of 4-6 nm are visible [Figure 1b]. This TEM image is overlapping of NPs gives approx. 90% smaller particles and around 10% needle like nanorods of IO NPs. The IO NPs were treated with silica precursor TEOS to obtained SIO NPs using three different amount of TEOS and keeping constant all other reagents and parameters. The higher amount (2.26 and 1.13 mmol) of silica precursor TEOS results in macro size of silica coated agglomerated particles (data not shown here) but using smaller amount (0.56 mmol) of TEOS results in 75 ± 10 nm SIO NPs as shown in Figure 1b. In this image the center black dots are IO NPs and surrounding gray color is comprised silica coating. The physical appearance of these SIO NPs is brown color.

VSM (DMS, 1660) magnetometer was used for the quantitative magnetization measurements of IO and SIO NPs which were compared with commercially available Dyna M-280 magnetic beads as shown in Figure 2a. The saturation magnetization (M_s , emu/g) and coercivity (H_c , Oe) obtained from these magnetic hysteresis loops (black curve) could be seen for the IO NPs. Due to the weight increased by non-magnetic silica, the M_s of SIO NPS were decreased by increasing the amount of silica used in the synthesis process. That is the reason for the differences between SIO NPs from 2a to 2c SIO NPs in Table 1. The SIO NPs 2c (blue curve) synthesized using 0.56 mmol of TEOS and used to capture *E. coli*, showed comparatively higher M_s , dropped by $\sim 67\%$ compared to IO NPs. Although SIO NPs synthesized here are not super paramagnetism due to their H_c were above 10 Oe. However, they possessed higher saturation magnetization over Dyna M-280 magnetic

NPs	M_s (emu/g)	H_c (Oe)
1	45.17	9.81
DB-M280	11.87	9.47
2a	7.88	15.26
2b	8.16	14.92
2c	15.08	13.38

Table 1: Saturation magnetization and coercivity values of IO and SIO NPs.

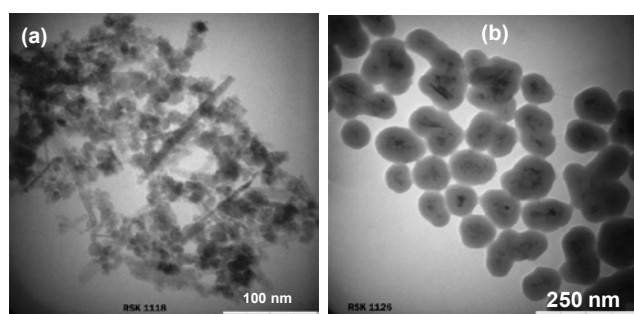


Figure 1: TEM images of (a) Iron oxide ($\text{Fe}_3\text{O}_4 + \text{Fe}_2\text{O}_3$) nanoparticles (IO-NPs), and (b) Silica coated Ironoxide ($\text{SiO}_2/\text{Fe}_3\text{O}_4 + \text{Fe}_2\text{O}_3$; SIO-NPs). Where the scale bar = 100 nm and 250 nm, respectively.

beads (DB-M280). The visual identification of magnetic property was characterized by applying external magnet outside of vial containing a suspension of SIO NPs. The Figure 2b (left vial) shows the suspended SIO NPs (0.5 mg/ml in PBS buffer (6.8 pH) and these SIO NPs were pulled from suspension through magnet Figure 2b (right vial).

To link SIO NPs 2 covalently with *E. coli* antibody, the hydroxyl groups of silica surface were chemically activated with CNBr. The CNBr reacts with the hydroxyl groups of silica in a mild basic medium to form cyanate esters and imidocarbonates [25], through electrophilic substitution reaction. These groups react with primary amine group of polyclonal *E. coli* antibody protein yielding an isourea and substituted imidocarbonates derivatives.

The yield the loading of antibody on the surface of SIO was calculated using a linear regression curve of the amount of antibody (5 - 75 μ g) vs. uv-visible absorption at 260 nm (data not shown here). The antibody-SIO conjugate was treated with 0.05M aq NaOH solution to cleave antibody from SIO NPs. The calculation results in ~20% loading of antibody on SIO NPs. This method is used to cleave isourea bonds (formed by cyanate ester and primary amine group) by the solvolytic attack of nucleophiles in the pH range 8-9.5 to release amino acid or protein [26].

The activated NPs 3 were characterized using FT-IR spectroscopy. Figure S11a shows FT-IR spectrum of SIO NPs 2, the characteristic spectrum of silica NPs with a broad band of hydroxyl group between 3000 - 3600 cm^{-1} . The activated particles 3 show a small band 2252.6 cm^{-1} for OCN group as shown in Figure S11b. The antibody linked NPs 4 were characterized using UV-vis absorption spectroscopy as shown in Figure S12. An absorption band between 265 - 285 nm was observed which shows similar absorption peak as *E. coli* antibody only. This FT-IR and UV-vis absorption spectra confirms that the NPs 4 are linked with antibody.

Capture of *E. coli*

Following the procedure described in section 2.8 the plates containing dilutions above 10^{-6} *E. coli* were overgrown and unable to be counted correctly. The 10^{-6} to 10^{-9} dilutions was mixed with immunomagnetic NPs 4 but the sample containing bacterial cells from 10^{-8} dilution (containing ~ 180 cfu/mL) was selected for further study. To confirm the capture of bacteria using immunomagnetic NPs 4, they were mixed with *E. coli* suspension and incubated for 30 min at RT. After washing NPs were placed on agar plate to incubate further 24 hr.

The agar plate in figure 3c shows incubated cfu/mL of *E. coli* from 10^{-8} dilution suspension, this was used to treat the NPs 4. The figure 3c and d, show plated containing NPs 2 and 3 respectively treated with *E. coli* cells. These two plates were used as a negative control for the sample, because they should not capture any bacterium. Since, they were not linked with *E. coli* antibody. The sample plated is shown in Figure 3f. The presence of *E. coli* cfu on this plate, confirm that the immunomagnetic NPs 4 are capturing the *E. coli* cells from its 10^{-8} dilution suspension and it is due to antibody binding with the bacterial cell wall receptors.

Further the capture efficiency of NPs 4 was calculated based on the figure 3. That shows the total amount of live bacteria added [~180 cfu; figure 3c] and the total captured active bacteria colony appeared [5 cfu; figure 3f] on agar plate. Then the capture efficiency of NPs 4 was calculated using the following formula:

$$\text{Capture efficiency of NP 4} = \frac{\text{Total captured active bacterial (cfu)} \times 100}{\text{Total active bacterial (cfu) added}}$$

That resulted the capture efficiency of NPs 4 for live bacteria was ~3%, however there would be a dead and non growing bacteria will also present, which were not counted.

Further, the capture of *E. coli* using NPs 4 was confirmed using fluorescent microscopic imaging as shown in Figure 4a-d. The *E. coli* were treated with green fluorescent dye from BacLight™ bacterial viability kit [22]. The Figure 4a shows dye labeled green rod shaped bacteria cells. While the NPs 2 and 3 were treated with *E. coli*, washed and then treated with the fluorescent dye, but they did not show the presence of bacteria Figure 4b and c respectively. The sample containing complex of immunomagnetic NPs 4 and *E. coli* shows presence of bacteria as shown in Figure 4d. The agar plate and fluorescent imaging results prove that the NPs 4 are binding with the *E. coli* and after magnetic separation and washing the bacteria were remain bound with the immunomagnetic NPs. The captured *E. coli* complex 6, which was incubated with Ag NPs ~5 h was also monitored using FE-SEM images. Figure 5a-d show different regions of dead and damaged *E. coli* cell sample, embedded with SIO NPs 4 and Ag NPs aggregates. These images clearly show the toxic effect of Ag NPs and therefore act as antibacterial nanomaterial.

SERS study

The captured *E. coli* and 4 complexes in PBS (7.2 pH) were treated with sodium citrate reduced colloidal Ag NPs with the size of 6±4 nm in diameter and incubated up to 22.5 h at RT. Three deferent concentrations of Ag NPs solution (1x, 3x, and 5x concentration) were systematically investigated for SERS. The 5x concentration of Ag NPs was indicated best result of SEM and SERS. The SEM images were

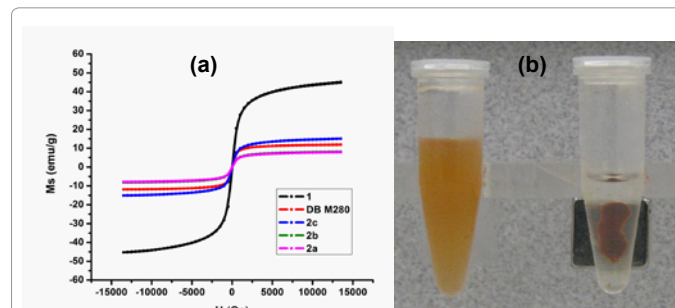


Figure 2: (a) Magnetic hysteresis graph of IO-NPs, commercial Dynal magnetic beads-M280 (DB-M280), and SIO-NPs, using three different amount of silica coating (b) left; camera photo of aqueous suspension of SIO-NPs and right: SIO-NPs separated from suspension using magnet.

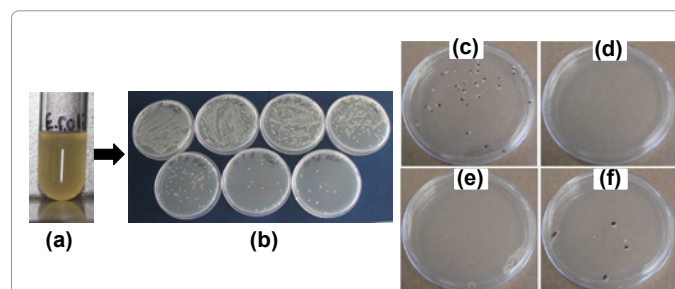


Figure 3: (a) Culture of *E. coli* suspension in LB growth media, (b) Agar growth plate showing *E. coli* cfu after incubation, which were plated from its 10^{-3} to 10^{-6} (top left to right) and 10^{-7} - 10^{-9} (bottom left to right) dilutions. Agar plating of capture and isolated *E. coli* from PBS suspension using NPs 4, where (c) is *E. coli* at 10^{-8} dilution, NPs (d) 2, (e) 3, (f) 4 incubated with *E. coli* at 10^{-8} dilution in PBS suspension.

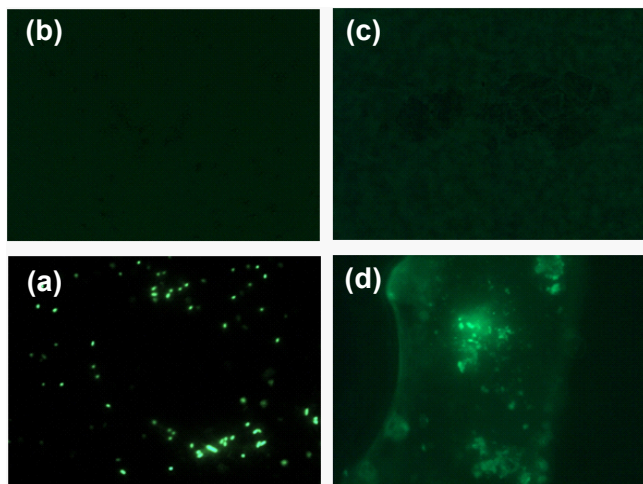


Figure 4: Fluorescent microscopic images of (a) *E. coli* only, NPs (b) 2, (c) 3, (d) 4 incubated with *E. coli* in PBS suspension.

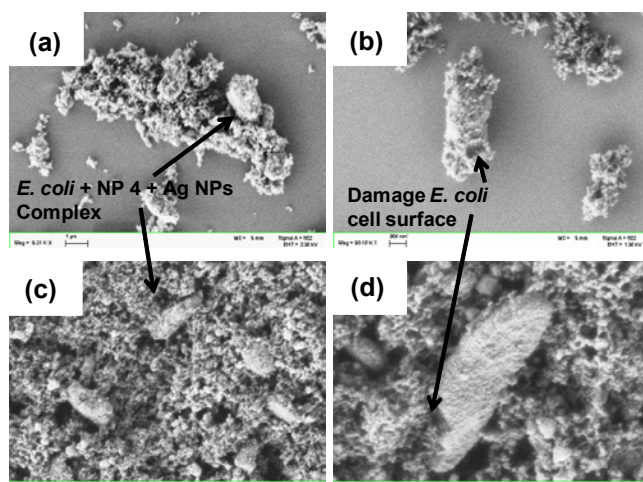


Figure 5: FE-SEM images of captured *E. coli* using *anti-E. coli* antibody functionalized magnetic nanoparticles 4 (a), (b), (c), and (d) four different images at different places of the sample.

taken at different spots of bacterial complex as shown Figure 5a-d. The Figure 5a,c shows isolated bacterial cells embedded with IM NPs and Ag NPs while image 5b,d are more focused to show the damage to the bacterial cells, that would cause its death. All four images were taken after 22.5 h of incubation with Ag NPs therefore the damage to the cells is clearly shows antibacterial property of the Ag NPs.

The SERS was performed on air dried samples placed on glass slide. Therefore, it is significant to study the background SERS signal which could interfere with sample signals. The Raman spectra of plain glass slide and SERS of NPs 3 and 4 are important to look first before the study of real samples and spectra of them serve as control. Figure 6a shows Raman spectra of plain glass slide. This corresponds with typical Raman spectra of sodium silicate glass framework. Dry glass shows major bands at 563, and 1105 cm^{-1} . Where the band at 1105 cm^{-1} is indicative of Si-O units and 563 cm^{-1} is associated with Si-O-Si linkage. The band appears around 470 cm^{-1} originates from the reminiscent of silica gel annealed at 200-400 $^{\circ}\text{C}$ [27]. There are obvious shoulders near

790 and 1000 cm^{-1} . Mysen et al. [28] de-convoluted that these band originate from hydrated sodium silicate glass [28].

Two NPs 2 and 4 were also selected for Raman spectroscopic analysis in the presence of 5X concentration of Ag NPs. Spectra of SIO NPs 2 is shown in Figure 6b. It consist three bands with position at about 354, 505 and 733 cm^{-1} and according to reported literature these spectra are associated with $\gamma\text{-Fe}_2\text{O}_3$ (maghemite) [29]. The spectral band at about 210, 398, 654 cm^{-1} are associated with the $\alpha\text{-Fe}_2\text{O}_3$ (hematite) phase of IO particles [30]. Silica coating of these IO NPs can be seen through band at 949 and 1287 cm^{-1} for $\text{O}_3\text{Si-OH}$ linkage [31,32]. Further, the Raman spectra of NPs 4 showed characteristic bands of proteins. A sharp peak for O-Ag bond vibration and interactions of ionic species, adsorbed onto Ag NPs can be seen at 241 cm^{-1} [33]. Bands at 560 and

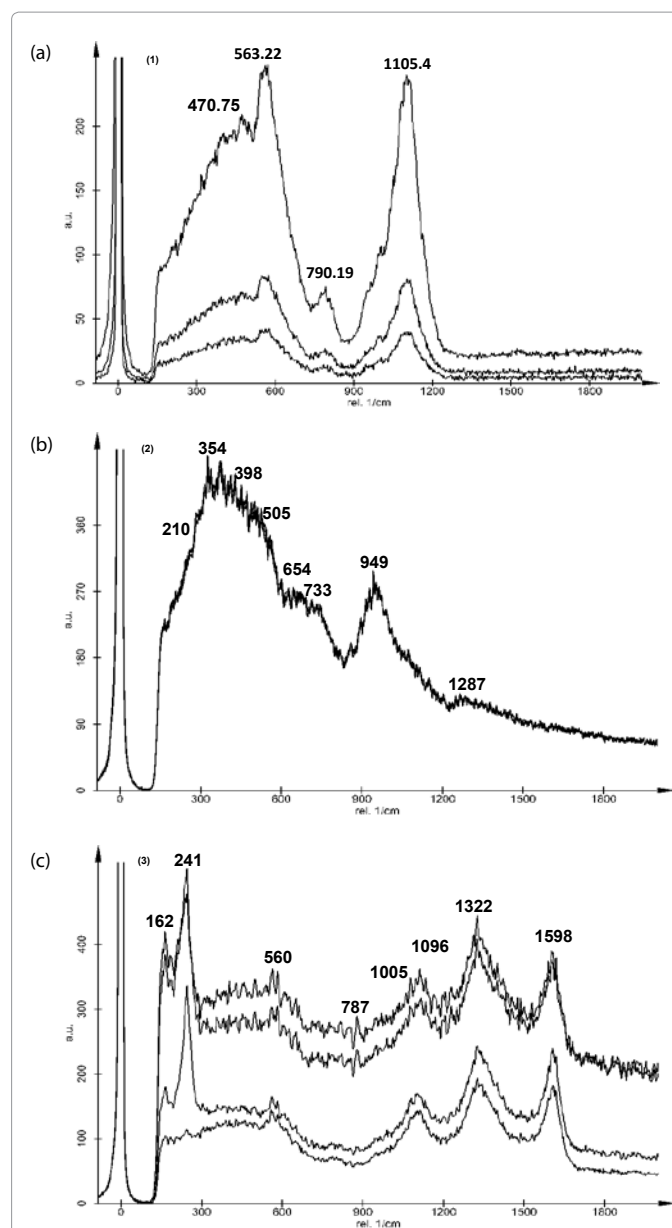


Figure 6: (a) Raman spectra of plain glass slide, SERS spectra of (b) SIO-NPs 2 in presence of colloidal Ag, (c) *anti-E. coli* antibody functionalized SIO-NPs 4 in presence of colloidal Ag.

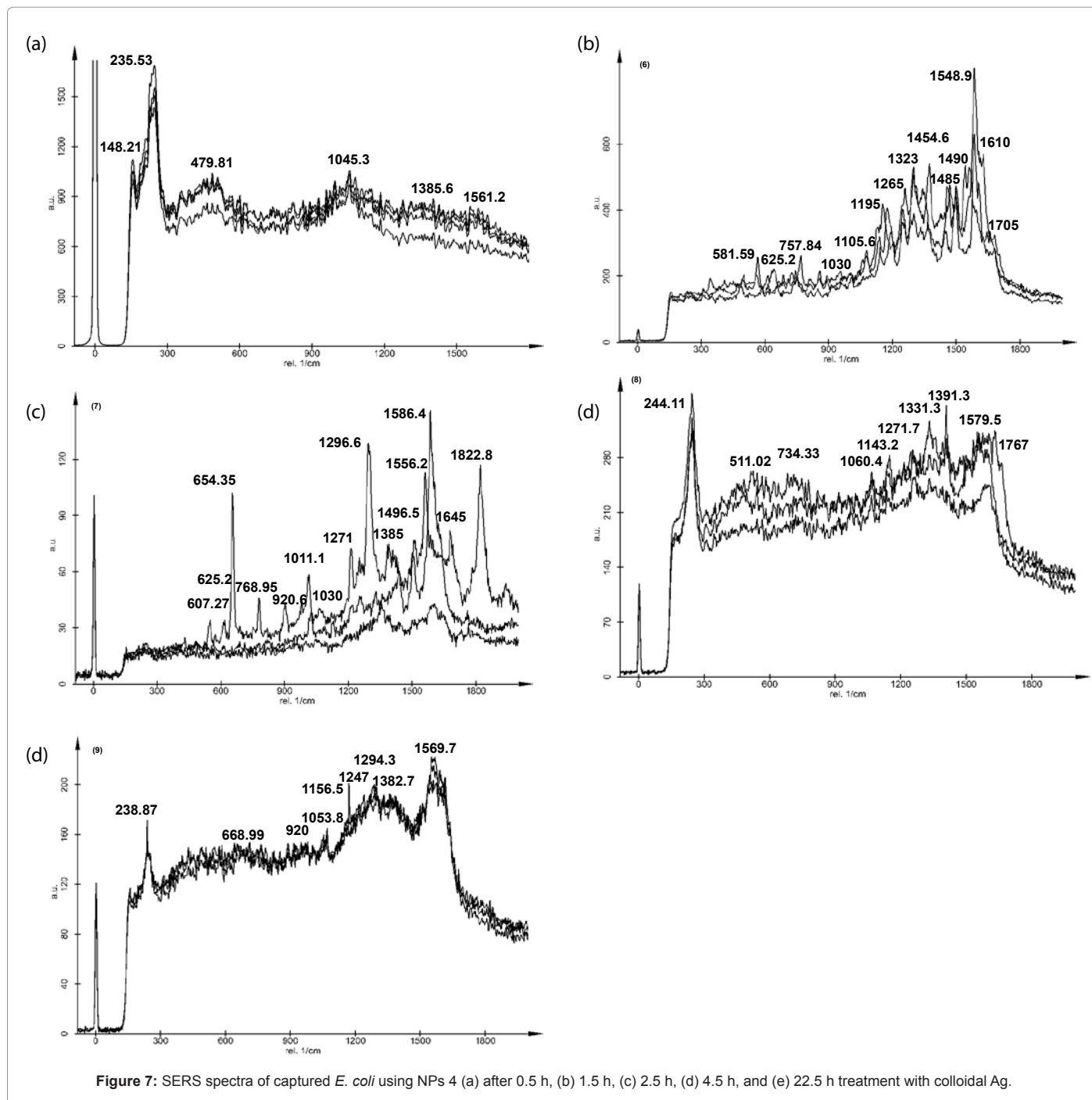


Figure 7: SERS spectra of captured *E. coli* using NPs 4 (a) after 0.5 h, (b) 1.5 h, (c) 2.5 h, (d) 4.5 h, and (e) 22.5 h treatment with colloidal Ag.

787 cm^{-1} are showing Si-O-Si linkage and Fe_2O_3 (maghemite) units of NPs similar to previous spectra. The characteristic SERS band for protein comes from phenyl vibration (around 1001 cm^{-1}), amide I, II and III vibrations (from 1100 to 1600 cm^{-1}) [34], these bands at 1005, 1096, 1322, and 1598 cm^{-1} can be seen in Figure 6c and are indicative of antibody attachment with NPs 4.

Time titration study of captured *E. coli*, was performed at the period of 0.5, 1.5, 2.5, 4.5 and 22.5 h of incubation of Ag NPs, the SERS spectra of the respective time period are shown in Figure 7a-e. It appears that Ag NPs dose not start reacting with bacterial cells in the

first 1.5 h of incubation. The spectra in Figure 7a is similar to IM NPs 4, corresponds to O-Ag, silica, and protein bands around 235, 479, 1045, 1385 and 1561 cm^{-1} . After 1.5 h of incubation with bacterial cells SERS give major signals for protein (1250 – 1370 cm^{-1}), lipids (1420 – 1550 cm^{-1}) and some nucleic acids (1550 – 1670 cm^{-1}) bands also. Some of the recent reports have well explained the SERS finger printing of these biomolecules from *E. coli* species [7,21,35]. These can be seen in Figure 7b. The weak band at 581 and 1030 cm^{-1} corresponds to carbohydrate, mainly -C-C-, C-O, and C-O-H skeleton [36,37]. The weak bands at 625 cm^{-1} for COO- group of protein, peptides and aminoacids. 1105 cm^{-1} band is from glass slide. 1195, 1265, and 1323 cm^{-1} bands are

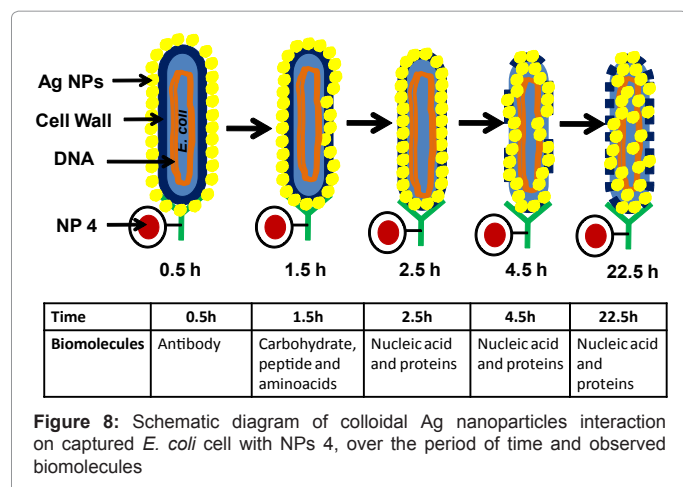


Figure 8: Schematic diagram of colloidal Ag nanoparticles interaction on captured *E. coli* cell with NPs 4, over the period of time and observed biomolecules

showing amide I and III for N-H [38], alkane CH_2 twist, rock mode, and C-H linkage [39] respectively. The $\delta(\text{CH}_2)$ from lipid group can be seen at 1454 cm^{-1} . Adenine and guanine band appears at around 1485 cm^{-1} . The band at about 1548 cm^{-1} comes from C=C (lipid), $\delta(\text{N-H})$ and $\nu(\text{C-N})$ from amide II group. Further weak signals at after 1600 to 1700 cm^{-1} are from nucleic acid [36,40]. SERS signal at 1.5 h indicate there diffusion of Ag NPs into the bacterial cell is happening and after 2.5 h of incubation SERS shows sharp and clear bands mainly of nucleic acids [41,42,43] as shown in Figure 7c. The peaks between 600 and 800 cm^{-1} and between 1500 and 1700 cm^{-1} attribute DNA or RNA inside the bacterium. Peak at 1011 cm^{-1} is expected to come from phenylalanine, 920 cm^{-1} from C-N stretch, 1030 cm^{-1} from carbohydrate. Peaks at 1271 , 1296 , and 1385 cm^{-1} would correspond to protein and peptides linkage. Peaks at 1556 cm^{-1} is showing lipid (C=C) region and peaks 1586 , 1645 , 1822 cm^{-1} etc are similar to bacterial DNA [36,39].

Longer incubation of bacteria with Ag NPs, Figure 7d shows spectra after 4.5 hr of incubation and indicates that the carbohydrate, protein – peptides and nucleic acid SERS band are present but comparatively in weaker intensity. Similarly the spectra after 22.5 h, as shown in Figure 7e correspond to protein and nucleic acid bands. From these two figures one can envision that the Ag NPs could enter more deeply into bacterial cell over the longer period of incubation.

Based on SERS spectral results, we made schematic diagram, as shown in Figure 8, of our hypothesis for stepwise interaction of Ag NPs with *E. coli* cells surface and its insertion inside the cell. This figure shows in starting Ag NPs were sitting outside of cell wall and over the period of incubation they start interacting with the deferent molecules of the cells and eventually they are completely inserted inside the cell. The SEM images [Figure 5b, d] also support the damage bacterial cell surfaces which allow to Ag NPs to be inserted.

Conclusion

In this paper, we demonstrate the synthesis of silica coated ironoxide nanoparticles (SIO NPs). These SIO NPs showed approximately 27% of saturation magnetization compared to commercially available magnetic beads. The SIO NPs were activated using cyanogens bromide and covalently linked with polyclonal *E. coli* antibody. The immuno NPs were used to capture and isolate *E. coli* from 180 cfu/mL aqueous suspension and treated with colloidal Ag NPs at 5X concentration. The SERS at five different period of time was performed; sharp and distinguished peaks were obtained in 2.5 to 4.5 h spectra. All the SERS spectra and SEM images show the identification of various

biomolecules of *E. coli* cell. The immune-magnetic isolation of bacterial cells for capture, concentration and SERS spectral analysis is a quick and reliable method for identification of bacterial species without extensive experiments and statistical data treatment.

Acknowledgment

The financial support from the U.S. Department of Agriculture (No. 2009-34479-19833, and 2010-34479-20715) and partially M. J. Murdock charitable trust for partner in science program (2009322: BAH: 2/25/2010) and the Center for Biological Applications of Nanotechnology (BANTech) group at the University of Idaho (UI) are gratefully acknowledged. The authors would like to thank Dr. Thomas J. Williams and Dr. Franklin Bailey (electron microscopy center facility at the UI) for providing TEM and SEM images.

References

- Thompson KC, Gray J, David P. Sartory (2004) Microbiological analysis: How soon we have the results? Water Contamination Emergencies. Can We Cope? The Royal Society of Chemistry 110-121
- Olson WP (2000) Automated microbial identification and quantitation: technologies for the 2000s. CRC Press.
- Stender H, Oliveira K, Rigby S, Bargoot F, Coull J (2001) Rapid detection, identification, and enumeration of *Escherichia coli* by fluorescence in situ hybridization using an array scanner *J Microbiol Methods* 45: 31-39.
- Johnson-White B, Lin B, Ligler FS (2004) Combination of Immunosensor Detection with Viability Testing and Confirmation Using the Polymerase Chain Reaction and Culture. *Anal Chem* 79: 140-146.
- Liu JC, Chen WJ, Li CW, Mong KKT, Tsai PJ, et al. (2009) Identification of *Pseudomonas aeruginosa* using functional magnetic nanoparticle-based affinity capture combined with MALDI MS analysis. *Analyst* 134: 2087-2094.
- Carter EA, Marshall CP, Ali MHM, Ganendren R, Sorrell TC (2007) Infrared Spectroscopy of Microorganisms: Characterization, Identification, and Differentiation. *New Approaches in Biomedical Spectroscopy*, ACS Symposium Series (chapter 6) 963: 64-84.
- Jarvis RM, Goodacre R (2008) Characterisation and identification of bacteria using SERS. *Chem Soc Rev* 37: 931-936.
- Guyen B, Akgul NB, Temur E, Tamer U, Boyacı IH (2011) SERS-based sandwich immunoassay using antibody coated magnetic nanoparticles for *Escherichia coli* enumeration. *Analyst* 136: 740-748.
- Premasiri WR, Moir DT, Klempner MS, Ziegler LD (2007) Surface-Enhanced Raman Scattering of Microorganisms. *New Approaches in Biomedical Spectroscopy*, ACS Symposium Series (chapter 12) 963: 164-185.
- Neng J, Harpster MH, Zhang H, Mecham JO, Wilson WC, et al (2010) A versatile SERS-based immunoassay for immunoglobulin detection using antigen-coated gold nanoparticles and malachite green-conjugated protein A/G. *Biosens Bioelectron* 26: 1009-1015.
- Kneipp J, Kneipp H, Wittig B, Kneip K (2010) Following the Dynamics of pH in Endosomes of Live Cells with SERS Nanosensors. *J Phys Chem C* 114: 7421-7426.
- Yan B, Reinhard BM (2010) Identification of Tumor Cells through Spectroscopic Profiling of the Cellular Surface Chemistry. *J Phys Chem Lett* 1: 1595-1598.
- Ravindranath SP, Wang Y, Irudayaraj J (2011) SERS driven cross-platform based multiplex pathogen detection. *Sens Actuators B Chem* 152: 183-190.
- Liu Y, Chao K, Nou X, Chen YR (2009) Feasibility of colloidal silver SERS for rapid bacterial screening. *Sens & Instrumen Food Qual* 3: 100-107.
- Das G, Gentile F, Coluccio ML, Cojoc G, F Mecarini (2011) Low Concentration Protein Detection Using Novel SERS Devices. *Opt Fluor Micros* 191-210.
- Efrima S, Zeiri L (2008) Understanding SERS of bacteria. *J Raman Spectrosc* 40: 277-288
- Durán N, Rosa MA, D'Annibale A, Gianfreda L (2002) Applications of laccases and tyrosinases (phenoloxidases) immobilized on different supports: a review. *Enzyme and Micro Tech* 31: 907-931.
- Brady D, Jordaan J (2009) Advances in enzyme immobilization. *Biotechnol Lett* 31: 1639-1650.
- Park HY, Schadt MJ, Wang L, Lim IS, Njoki PN, et al. (2007) Fabrication of

- Magnetic Core@Shell Fe Oxide@Au Nanoparticles for Interfacial Bioactivity and Bio-separation. *Langmuir* 23: 9050–9056.
20. Liu Y, Chen YR, Nou X, Chao K (2008) Potential of surface-enhanced Raman spectroscopy for the rapid identification of *Escherichia coli* and *Listeria monocytogenes* cultures on silver colloidal nanoparticles. *Appl Spectrosc* 61: 824-31.
21. Kahraman M, Yazici MM, Sahin F, Culha M (2008) Convective Assembly of Bacteria for Surface Enhanced Raman Scattering. *Langmuir* 24: 894-901.
22. Rastogi SK, Handricks VJ, Gibson CM, Newcombe D, Branen JR, et al. (2011) Ag colloids and Ag Clusters over EDAPTMS-Coated Silica Nanoparticles: Synthesis, Characterization and Antibacterial Activity against *Escherichia coli*. *Nanomedicine* 7: 305-314.
23. Tada M, Hatanaka S, Sanbonsugi H, Matsushita N, Abe M (2003) Method for synthesizing ferrite nanoparticles 30 nm in diameter on neutral pH condition for biomedical applications. *J Appl Phys* 93: 7566-7569.
24. Kang YS, Risbud S, Rabolt JF, Stroeve P (1996) Synthesis and Characterization of Nanometer-Size Fe_3O_4 and $\gamma-Fe_2O_3$ Particles. *Chem Mater* 8: 2209–2211.
25. Jurado LA, Mosley J, Jarrett HW (2002) Cyanogen bromide activation and coupling of ligands to diol-containing silica for high-performance affinity chromatography optimization of conditions. *J Chromatogr A* 971: 95-104.
26. Kennedy JF, Barnes JA, Matthews JB (1983) Mechanism of reaction of cyanogen bromide-activated agarose with amines and the solvolysis of amine ligands. *Polymer International* 15: 133-138.
27. McMillan PF, Remmele RL Jr (1986) Hydroxyl Sites in SiO_2 glass: A Note on Infrared and Raman Spectra. *Amer Miner* 71: 772-778.
28. Mysen BO, Virgo D, Seifert FA (1982) The structures of silicate melts: Implication of Chemical and Physical Properties of Natural Magma. *Rev Geophys Space Phys* 20: 353-383.
29. Boucherit N, Goff AH, Joiret S (1991) Raman studies of corrosion films grown on Fe and Fe-6Mo in pitting conditions *Corros Sci* 32: 497-507.
30. Pérez-Robles F, García-Rodríguez FJ, Jiménez-Sandoval S, González-Hernández J (1990) Raman study of copper and iron oxide particles embedded in an SiO_2 matrix. *J Raman Spectrosc* 30: 1099-1104.
31. Humbert B, Burneau A, Gallas JP, Lavalley JC (1992) Origin of the Raman bands, D_1 and D_2 , in high surface area and vitreous silicas. *J Non-Crystal Solids* 143: 75-83.
32. Riegel B, Hartmann I, Kiefer W, Groß J, Fricke J (1997) Raman spectroscopy on silica aerogels. *J Non-Cryst Solids* 211: 294-298.
33. Canameres MV, Garcia-Ramos JV, Go´mez-Varga JD, Domingo C, Sanchez-Cortes S (2005) Comparative Study of the Morphology, Aggregation, Adherence to Glass, and Surface-Enhanced Raman Scattering Activity of Silver Nanoparticles Prepared by Chemical Reduction of Ag^+ Using Citrate and Hydroxylamine. *Langmuir*. 21: 8546-8553.
34. Guicheteau JA, Gonser K, Steven CD (2004) Raman and Surface Enhanced Raman of Biological Material.
35. Naja G, Bouvrette P, Champagne J, Brousseau R, Luong JHT (2010) Activation of Nanoparticles by Biosorption for *E.coli* Detection in Milk and Apple Juice. *Appl Biochem Biotech* 162: 460-475.
36. Delfino I, Camerlingo C, Portaccio M, Ventura BD, Mita L, et al. (2011) Visible micro-Raman spectroscopy for determining glucose content in beverage industry. *Food Chem* 127: 735-742.
37. Maquelin K, Choo-Smith LP, Vreeswijk TV, Endtz HP, Smith B, et al. (2000) Raman Spectroscopic Method for Identification of Clinically Relevant Microorganisms Growing on Solid Culture Medium. *Anal Chem* 72: 12-19.
38. Schuster KC, Reese I, Urlaub E, Gapes JR, Lendl B (2000) Multidimensional Information on the Chemical Composition of Single Bacterial Cells by Confocal Raman Microspectroscopy. *Anal Chem* 72: 5529-5534.
39. Venkatakrishna K, Kurien J, Pai KM, Valiathan M, Kumar NN, et al. (2001) Optical Pathology of oral tissues: A Raman spectroscopy diagnostic method. *Current Sci* 80: 665-669.
40. Zheng YG, Carey PR, Palfey BA (2004) Raman spectrum of fully reduced flavin. *J Raman Spectrosc* 35: 521-524.
41. Goodacre R, éadaoin MT, Burton R, Kaderbhai N, Woodward Am, et al. (1998) Rapid identification of urinary tract infection bacteria using hyperspectral whole-organism fingerprinting and artificial neural networks. *Microbiol* 144: 1157-1170.
42. Naumann D (2001) FT-Infrared and FT-Raman Spectroscopy in Biomedical Research. *Appl Spectro Rev* 36: 239-299.
43. Maquelin K, Kirschner C, Choo-Smith LP, Braak VVD, Endtz HP, et al. (2002) Identification of medically relevant microorganisms by vibrational spectroscopy. *J Microbio Methods* 51: 255-271.